ISSN 1067-8212, Russian Journal of Non-Ferrous Metals, 2018, Vol. 59, No. 4, pp. 385–392. © Allerton Press, Inc., 2018.

FOUNDRY

Effects of Indium Content on Microstructural, Mechanical Properties and Melting Temperature of SAC305 Solder Alloys[1]

Phairote Sungkhaphaitoon[a, *] and Suchart Chantaramanee[b]

[a] *Department of Materials Science and Technology, Faculty of Science, Prince of Songkla University, Hat Yai, Thailand*

[b] *Department of Industrial Engineering, Faculty of Engineering, Rajamangala Unversity of Technology, Srivijaya Songkhla, Thailand*

**e-mail: phairote.s@psu.ac.th*

Received November 16, 2017

Abstract—The present study investigated the effects of indium (In) addition on the microstructure, mechanical properties, and melting temperature of SAC305 solder alloys. The indium formed IMC phases of $Ag_3(Sn,In)$ and $Cu_6(Sn,In)_5$ in the Sn-rich matrix that increased the ultimate tensile strength (UTS) and the hardness while the ductility (% EL) decreased for all In containing solder alloys. The UTS and hardness values increased from 29.21 to 33.84 MPa and from 13.91 to 17.33 HV. Principally, the In-containing solder alloys had higher UTS and hardness than the In-free solder alloy due to the strengthening effect of solid solution and secondary phase dispersion. The eutectic melting point decreased from 223.0°C for the SAC305 solder alloy to 219.5°C for the SAC305 alloy with 2.0 wt% In. The addition of In had little effect on the solidus temperatures. In contrast, the liquidus temperature decreased with increasing In content. The optimum concentration of 2.0 wt % In improved the microstructure, UTS, hardness, and eutectic temperature of the SAC305 solder alloys.

Keywords: SAC305 solder alloys, ultimate tensile strength, hardness, intermetallic compound, eutectic melting point

DOI: 10.3103/S1067821218040120

INTRODUCTION

Owing to the unique properties of the materials, conventional soldering processes have for many years used a Sn–Pb system. However, medical studies have shown that Pb is a heavy metal toxin that can damage kidney, liver, blood, and the central nervous system [1, 2]. Therefore, research has been conducted into Pb-free solder alloys with the right balance of thermal, mechanical, and soldering properties to replace Sn–Pb solder alloys. Interest has rapidly increased in Sn–Ag–Cu (SAC) solder alloys containing more than 3.0 wt % Ag, such as SAC305, SAC307, and SAC405, as their relatively good solderability has made these alloys the most promising alternatives in microelectronic applications [3]. However, the drawbacks of these alloys include short creep rupture lifetimes and relatively high melting points. Also, the formation of intermetallic compounds (IMCs) of Ag_3Sn and Cu_6Sn_5 in the solder matrix impairs the mechanical properties of the solder [4]. For these reasons, metal additives such as Bi, In, Ga, Zn, and Fe and nanoparticles such as Al_2O_3, TiO_2, and ZnO have been introduced into SAC solder alloys in order to improve their microstructure, and their mechanical and thermal properties [5–10]. In the case of indium, the addition of 9.0 wt% In into Sn–3.5Ag–0.5Cu solders led to the formation of $Cu_6(Sn,In)_5$ and $Ag_3(Sn,In)$ precipitates embedded in the β-Sn matrix [11]. This result was in good agreement with other reports [12, 13]. The addition of 0.5–3.0 wt% In into Sn–0.3Ag–0.7Cu solders led to the more uniform distribution of intermetallic compounds and increased the tensile strength and microhardness [5, 14]. Moreover, the solidus and liquidus temperatures of solders were lowered as a function of the In content [5, 15, 16]. For example, the melting temperature of Sn–10Sb solder alloy was reduced by the addition of 0.5–2.0 wt % In and the solidus and liquidus temperatures decreased as the In content increased [15]. The present paper further investigates the influence of indium on the microstructure, mechanical properties, and melting temperature of SAC305 solder alloys for industrial electronics applications.

[1] The article is published in the original.

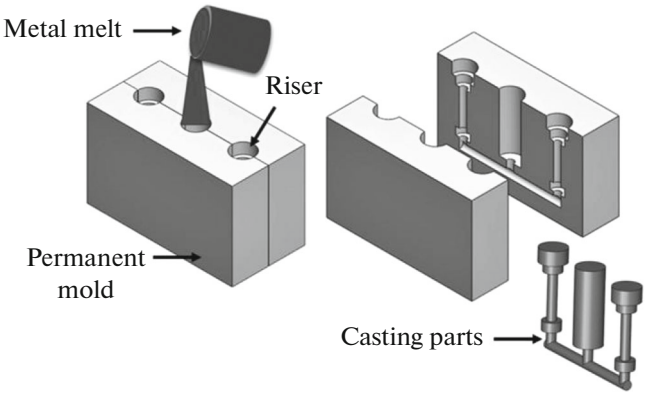

Fig. 1. Schematic of gravity casting process of the solder alloys.

EXPERIMENTAL

The formulations of the solder alloys used in the experiment were SAC305, SAC305–0.5In, SAC305–1.0In, and SAC305–2.0In. The purities of the raw materials used were 99.995, 99.999, 99.995 and 99.999% for Sn, Ag, Cu, and In respectively. To commence the experiment the raw materials were placed into a graphite crucible and melted in an electric resistance furnace at 400°C for 24 h to ensure complete dissolution of the Sn, Cu, Ag and In elements. In the laboratory, an electric resistance furnace was fabricated capable of melting 5 kg of Sn-based solder alloy per batch. Before the casting processes began, the temperature of the molten alloy was reduced to 270°C. After preheating the permanent mold to 220°C, the molten alloy from the graphite crucible was poured into the permanent mold. The permanent mold gravity casting process is shown in Fig. 1. The as-cast molten alloys, when completely solidified at ambient temperature, were removed from the permanent mold. The chemical compositions of the four solder alloys were characterized by X-ray fluorescence spectrometry (XRF, PW2400, Philips). The results of the characterizations are shown in Table 1. For tensile testing, the as-cast specimens were cut, in accordance with ASTM E8 specifications, with a reduced section 6 mm in diameter and 30 mm in length. Before characterizing the microstructure and hardness of the solder alloys, the as-cast specimens were cut into small pieces, molded, polished, and then etched for 5 s with a solution of 5% HNO_3, 92% CH_3OH and 3% HCl. The microstructure of the solder alloys was characterized by scanning electron microscopy (SEM, Quanta 400, FEI). Phase identification was analyzed by energy dispersive X-ray spectroscopy (EDX). The hardness of the solder alloys was evaluated using the Vickers microhardness testing procedure (INNOVATEST, NOVA 130/240) at a constant load of 1.96 N and dwell time of 10 s. The final value was the average result of five hardness tests. The melting temperature of the solder alloys was determined by differential scanning calorimetry (DSC, NETZSCH, DSC 200 F3 Maia). The test was performed under argon (Ar) at a constant heating rate of 10°C/min. The tensile tests were carried out using a universal testing machine (UTM, Instron 5569) at a constant strain rate of 1.5 mm/min at room temperature. The value for the ultimate tensile strength of each alloy was obtained by averaging five test results.

Table 1. Chemical composition of the solder alloys

Solder alloys	Composition, wt %			
	Ag	Cu	In	Sn
Sn–3.0Ag–0.5Cu	3.68	0.41	–	balance
Sn–3.0Ag–0.5Cu–0.5In	3.67	0.48	0.64	balance
Sn–3.0Ag–0.5Cu–1.0In	3.36	0.44	1.21	balance
Sn–3.0Ag–0.5Cu–2.0In	3.43	0.47	2.28	balance

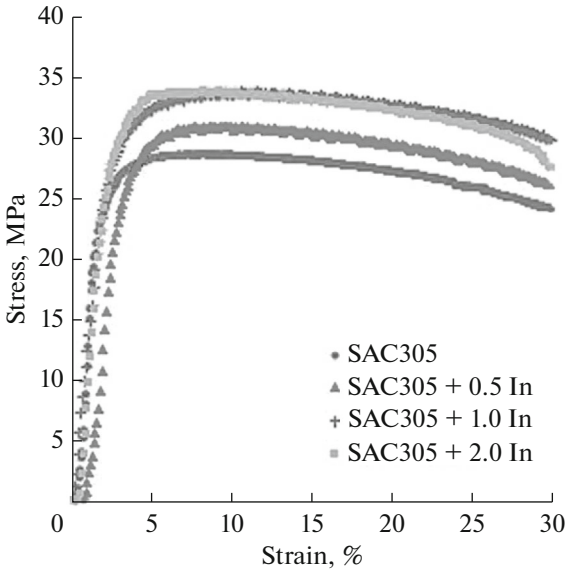

Fig. 2. The stress-strain curves of the solder alloys.

RESULTS AND DISCUSSION

Mechanical Properties of Solder Alloys

The stress-strain curves of the tensile tests of the solder alloys at a constant strain rate of 1.5 mm/min at room temperature are shown in Fig. 2. Increasing the In content increased the strength of the solder alloys. Figures 3a, 3b shows the effect of In content on the ultimate tensile strength (UTS), ductility (%EL), and hardness of the solder alloys. It is evident that increments of In content enhanced the UTS and the hardness while the %EL decreased for all In containing solder alloys. The UTS, hardness and %EL of the SAC305 solder alloy were 29.21 MPa, 13.91 HV and

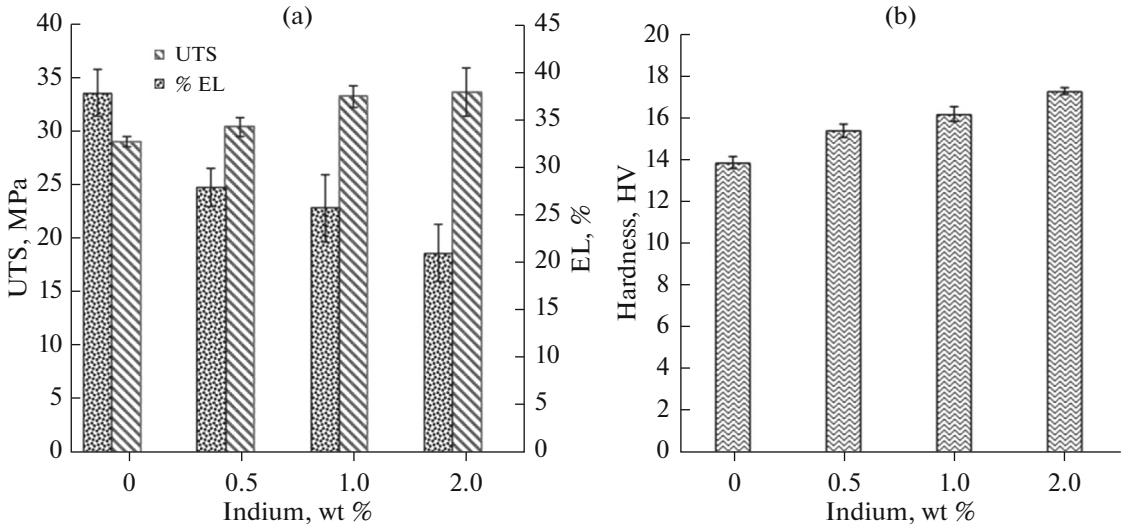

Fig. 3. Effect of In content on the mechanical properties of solder alloys: (a) ultimate tensile strength (UTS), ductility (%EL) and (b) hardness.

38%, whereas the UTS, hardness and %EL of the SAC305–2.0In solder alloy were 33.84 MPa, 17.33 HV and 21%, respectively. The increases in UTS and hardness of the solder alloys were attributed to the strengthening effect of solid solution and secondary phase dispersion [12, 15]. The addition of 0.5, 1.0, and 2.0 wt % In resulted in the formation of embedded $Ag_3(Sn,In)$ and $Cu_6(Sn,In)_5$ IMCs distributed throughout the Sn-rich matrix. The IMCs in the Sn-rich matrix inhibited the motion of dislocation. This led to the improvement of the UTS and hardness of the solder alloys [5, 12, 15].

Microstructure of Solder Alloys

The microstructures of the solder alloys were characterized by scanning electron microscopy (SEM). Figure 4a shows that the microstructure of the initial SAC305 solder alloy was composed of a β-Sn phase, and uniformly distributed small eutectic IMCs of Ag_3Sn and Cu_6Sn_5 [5, 12]. Figures 4b–4d shows that the microstructure of the SAC305–*x*In (x = 0.5, 1.0, and 2.0 wt %) solder alloy consisted of a β-Sn phase, and a needle-like structure of coarse eutectic IMCs. Comparing the microstructure with those presented in Fig. 4a, it was found that the addition of In resulted in a coarsening of the eutectic IMCs, especially of the Ag_3Sn and Cu_6Sn_5 IMCs. The Ag_3Sn and Cu_6Sn_5 IMCs were not only reduced in the number with increments of In content, but also changed to $Ag_3(Sn,In)$ and $Cu_6(Sn,In)_5$ IMCs. The formation of $Ag_3(Sn,In)$ and $Cu_6(Sn,In)_5$ IMCs was confirmed by EDX analysis. These results are consistent with those reported for Sn–0.7Cu–2Ag–2In, and Sn–3Ag–2Sb–*x*In (x = 1, 5, and 7 wt %) solder alloys [12, 17].

Figure 5 shows EDX mapping images of the elemental distribution in the SAC305 solder alloy. The green and pink areas are Ag and Cu phases uniformly interspersed between β-Sn phases (red areas). Figure 6 shows the distribution of Sn, Ag, Cu, and In in the SAC305–2.0In solder alloy. Embedded in the Sn-rich matrix, the red areas are Sn phases, the blue areas are Ag phases, the green areas are Cu phases, and the purple areas are In phases. The phase compositions of SAC305 and SAC305–2.0In solder alloys are presented in Fig. 7. Only the Ag_3Sn and Cu_6Sn_5 IMCs were present in the SAC305 solder alloy and the results of the EDX analysis are shown in Fig. 7a,b. The intermetallic compounds in the SAC305-2.0In solder alloy were $Ag_3(Sn,In)$ and $Cu_6(Sn,In)_5$. The EDX analysis shows that the compositions of the intermetallic phases were 40.3 wt % Ag, 56.0 wt % Sn, 3.7 wt % In, and 36.1 wt % Cu, 62.7 wt % Sn, 1.2 wt % In. The results of the analysis are presented in Figs. 7c, 7d and are also summarized in Table 2. These new intermetallic compound phases that formed in the β-Sn matrix could improve the mechanical properties of the solder alloys, particularly their tensile strength and microhardness [5, 12].

Table 2. The EDX determination of chemical composition of SAC305 and SAC305+2.0In solder alloys by wt %

Elements	Intermetallic compounds, wt %			
	Ag_3Sn	Cu_6Sn_5	$Ag_3(Sn,In)$	$Cu_6(Sn,In)_5$
Sn	50.9	69.7	56.0	62.7
Ag	49.1	–	40.3	–
Cu	–	32.1	–	36.1
In	–	–	3.7	1.2

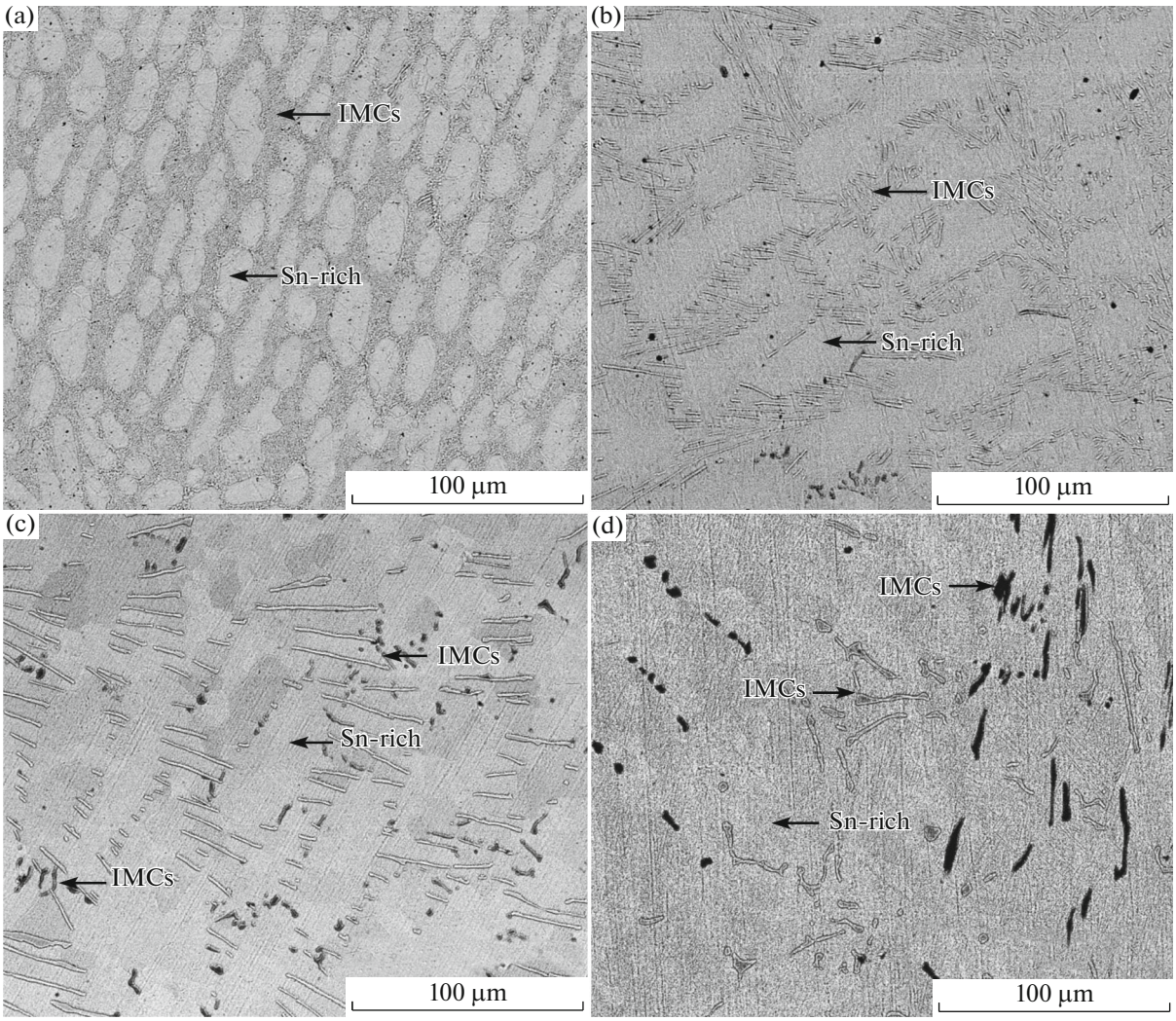

Fig. 4. SEM images of SAC305 alloys with different In contents: (a) 0%, (b) 0.5%, (c) 1.0%, and (d) 2.0%.

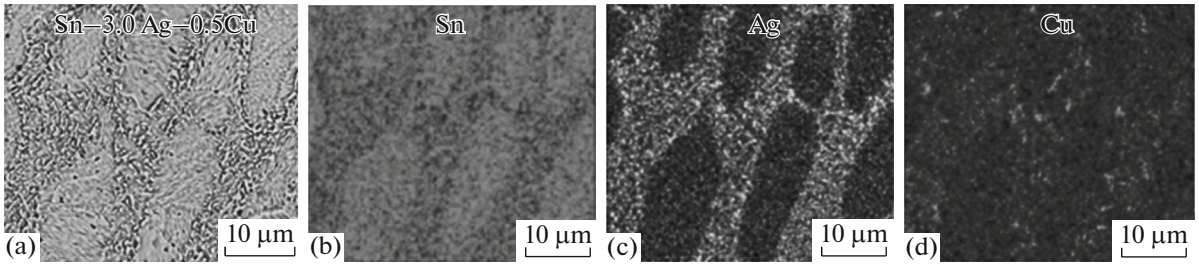

Fig. 5. EDX mapping images of elemental distribution: (a) SAC305, (b) Sn, (c) Ag, and (d) Cu.

Melting Temperature of Solder Alloys

The thermodiagrams of the four solder alloys during heating and cooling are shown in Fig. 8. The DSC results are summarized in Tables 3 and 4. During heating, the melting point (T_m) of the SAC305 solder alloys tended to decrease as the In content increased. The curve of the SAC305 solder alloy presents only one endothermic peak at 223.0°C, which is in good agreement with the melting procedure of SAC305 solder alloys [18, 19]. The addition of 0.5, 1.0 and 2.0 wt % In, reduced the melting point of SAC305 solder alloys from 223.0 to 219.5°C due to the formation of a new eutectic phase, and similar results have been reported when indium was added into other groups of solder

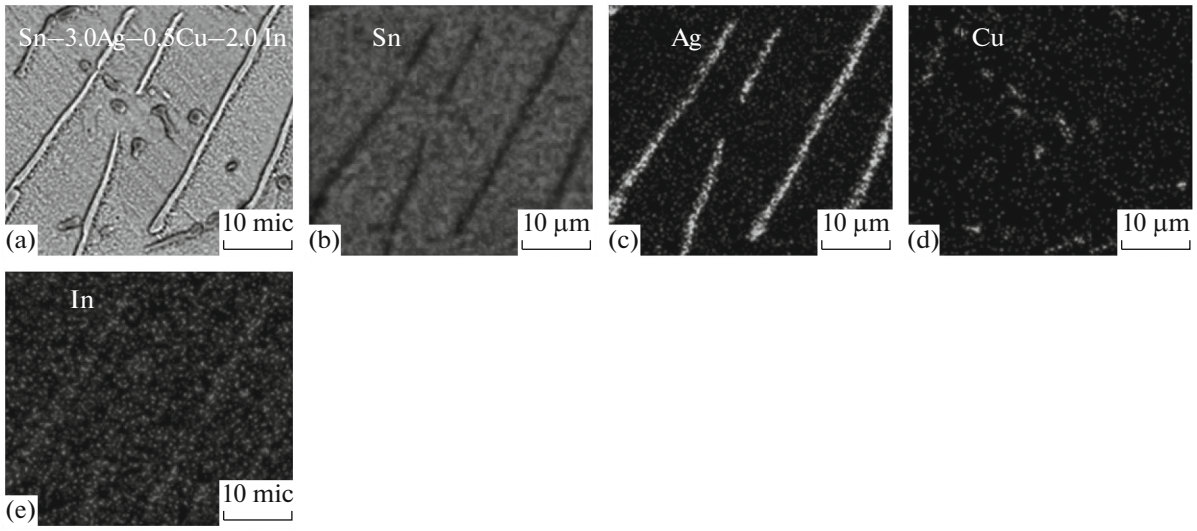

Fig. 6. EDX mapping images of elemental distribution: (a) SAC305–2.0In, (b) Sn, (c) Ag, (d) Cu, and (e) In.

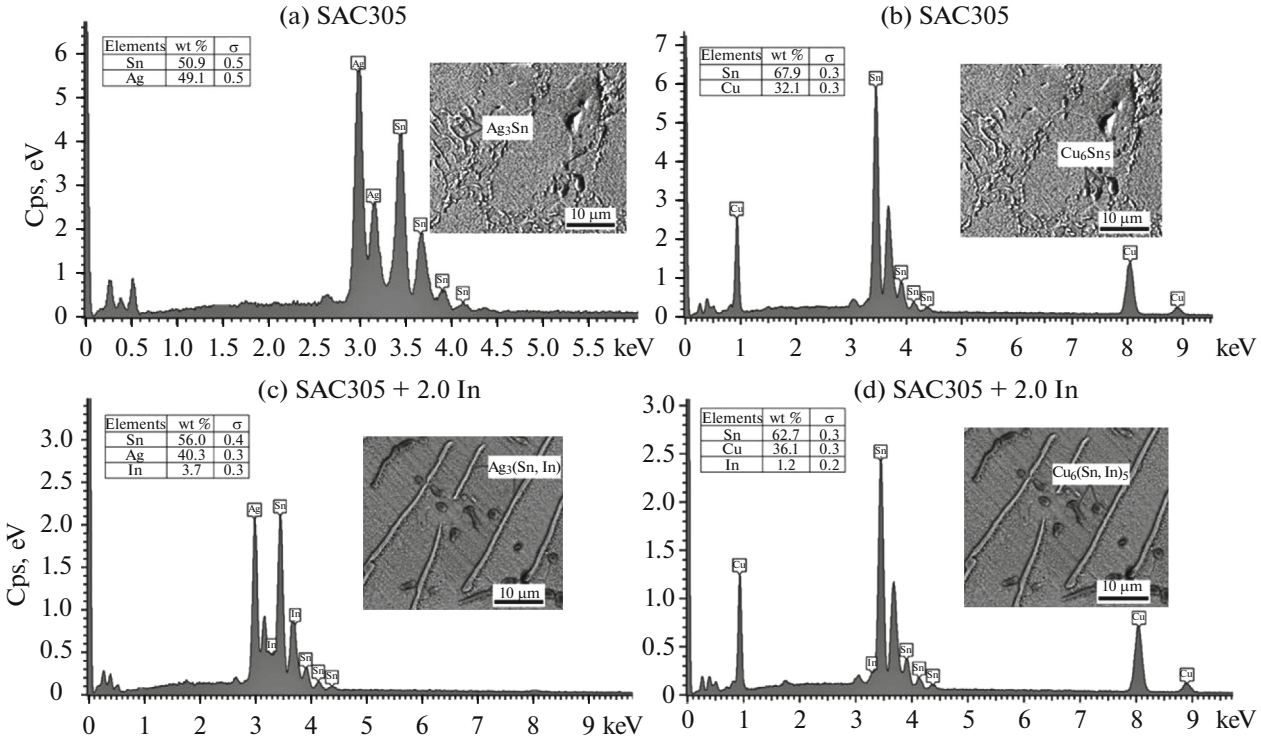

Fig. 7. SEM-EDX analysis of intermetallic compounds (IMCs): (a–b) SAC305, and (c–d) SAC305–2.0In.

alloys [5, 15, 17, 20, 21]. Table 3 shows that the addition of 0.5, 1.0 and 2.0 wt % In had a small effect on the solidus temperatures. On the other hand, the liquidus temperature decreased with increasing In content. These results are consistent with those reported for SAC0307, Sn–10Sb, Sn–3.5Ag, and Sn–3Ag–2Sb solder alloys [5, 15–17]. The solidus-liquidus range is very important for electronic applications. Normally, a good lead-free solder alloy has a small gap between the solidus and liquidus temperature (solidification ranges). The recommended solidification range for lead-free solders is not more than 30°C. Lead-free solder alloys with solidification ranges greater than 30°C may lead to soldering problems [17]. In Table 3, the solidification ranges of the In-containing solder alloys were smaller than the solidification ranges of Sn–

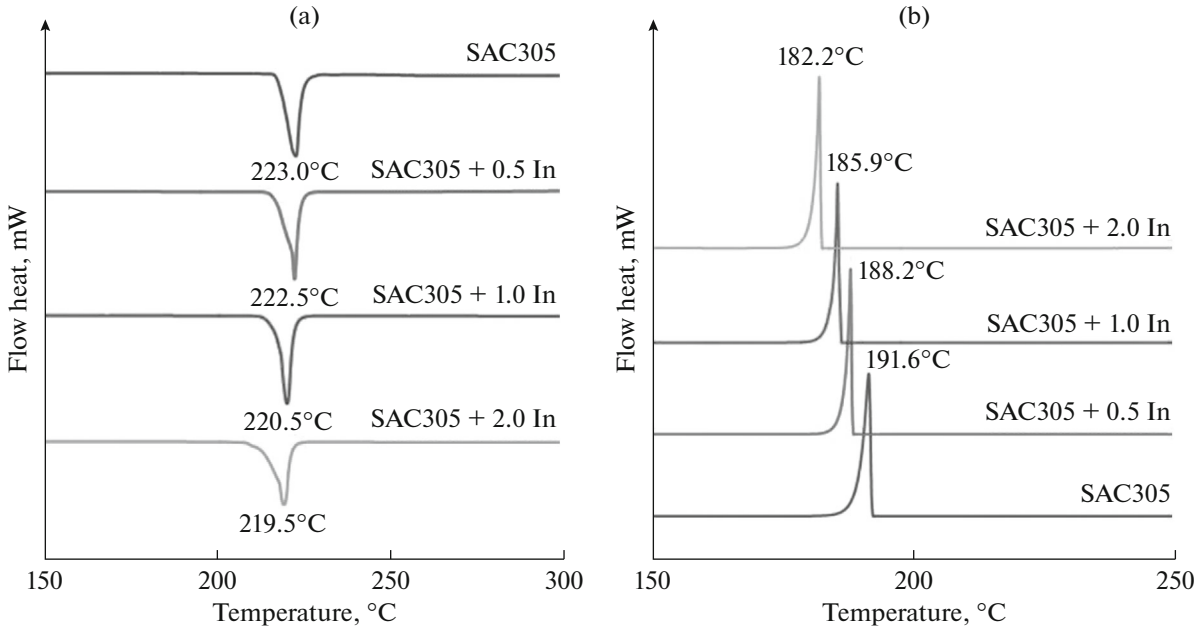

Fig. 8. DSC curves for the four alloys during (a) heating (endothermal) and (b) cooling (exothermal).

37Pb eutectic [22, 23]. Therefore, the addition of In elements could reduce the melting point and solidification ranges of SAC305 solder alloys. In addition, the undercooling of the In-containing solder alloys increased with higher In additions as shown in Table 4. The degree of undercooling is related to the nucleation and solidification of solder alloys. The difficult nucleation of the β-Sn phase during the solidification of Sn and Sn-based lead-free solder alloys can result in high degrees of undercooling of the liquid prior to solidification. That is to say, the β-Sn phase requires a large degree of undercooling in order to nucleate and solidify [24]. Therefore, the solder alloys that contained 0.5–2.0 wt % In produced larger grains in the β-Sn phase because of the significant degree of undercooling that occurred in comparison with the SAC305 sol-

Table 3. Comparison of melting point (T_m), solidus temperature (T_{onset}), liquidus temperature (T_{end}), solidification range (ΔT) of solder alloys

Solder alloys	T_m, °C	T_{onset}, °C	T_{end}, °C	$\Delta T = T_{end} - T_{onset}$,°C	Ref.
Sn–37Pb	183.0	179.5	191.0	11.5	[21]
SAC305	223.0	218.0	224.8	6.8	study
SAC305 + 0.5In	222.5	221.2	224.1	2.9	study
SAC305 + 1.0In	220.5	217.9	222.3	4.4	study
SAC305 + 2.0In	219.5	217.0	221.5	4.5	study

Table 4. Comparison of solidus temperature (T_{onset}) during heating, liquidus temperature (T_{onset}) during cooling and undercooling range of solder alloys

Solder alloys	(T_{onset}) heating, °C	(T_{onset}) cooling, °C	Undercooling ($T_{heating} - T_{cooling}$), °C
SAC305	218.0	192.2	25.8
SAC305 + 0.5In	221.2	188.4	32.8
SAC305 + 1.0In	217.9	186.2	31.7
SAC305 + 2.0In	217.0	182.5	34.5

der alloy (see in Fig. 4), and these results were consistent with previous reports [25, 26].

CONCLUSIONS

This paper studied the effects of indium addition on the microstructure, ultimate tensile strength, ductility, hardness and eutectic temperature of SAC305 solder alloys.

(i) The addition of indium into SAC305 solder alloys led to microstructural improvements, and the formation of new IMC phases of $Ag_3(Sn,In)$ and $Cu_6(Sn,In)_5$ in the β-Sn matrix. These phases could improve the mechanical properties of solder alloys.

(ii) The ultimate tensile strength and hardness of the SAC305 solder alloy increased when indium was added, rising from 29.21 MPa and 13.91 HV, respectively, for SAC305, to maximum values of 33.84 MPa and 17.33 HV for SAC305-2.0In.

(iii) The indium additions resulted in a decrease of the eutectic temperature of the SAC305 alloy from 223.0 to 219.5.2°C and solidification range values lower than the solidification range values of Sn-37Pb solder alloys.

(iv) The good properties of the solder alloys fabricated in these studies and the absence of lead in their composition make the developed materials suitable replacements for traditional Sn–Pb solders in electronics applications.

ACKNOWLEDGMENTS

This work was supported by Prince of Songkla University Research Fund (Fiscal Year 2016) under Grant number SCI590647S. In addition, we would like to thank academician Thomas Duncan Coyne for commenting and improving the English in the manuscript.

REFERENCES

1. Kotadia, H.R., Mokhtari, O., Clode, M.P., Green, M.A., and Mannan, S.H., Intermetallic compound growth suppression at high temperature in SAC solders with Zn addition on Cu and Ni–P substrates, *J. Alloy Compd.*, 2012, vol. 511, pp. 176–188.
2. Chang, S.Y., Jain, C.C., Chuang, T.H., Feng, L.P., and Tsao, L.C., Effect of addition of TiO_2 nanoparticles on the microstructure, microhardness and interfacial reactions of Sn3.5AgxCu solder, *Mater. Des.*, 2011, vol. 32, pp. 4720–4727.
3. Zhang, L., Xue, S.B., Zeng, G., Gao, L.L., and Ye, H., Interface reaction between SnAgCu/SnAgCuCe solders and Cu substrate subjected to thermal cycling and isothermal aging, *J. Alloy Compd.*, 2012, vol. 510, pp. 38–45.
4. Lin, F., Bi, W., Ju, G., Wang, W. and Wei, X., Evolution of Ag_3Sn at Sn–3.0Ag–0.3Cu–0.05Cr/Cu joint interfaces during thermal aging, *J. Alloy Compd.*, 2011, vol. 509, pp. 6666–6672.
5. Kanlayasiri, K., Mongkolwongrojn, M., and Ariga, T., Influence of indium addition on characteristics of Sn–0.3Ag–0.7Cu solder alloy, *J. Alloy Compd.*, 2009, vol. 485, pp. 225–230.
6. Mahdavifard, M.H., Sabri, M.F.M., Shnawah. D.A., Said, S.M., Badruddin, I.A., and Rozali, S., The effect of iron and bismuth addition on the microstructural, mechanical, and thermal properties of Sn–1Ag–0.5Cu solder alloy, *Microelectron. Reliab.*, 2015, vol. 55, pp. 1886–1890.
7. Mehrabi, K., Khodabakhshi, F., Zareh, E., Shahbazkhan, A., and Simchi, A., Effect of alumina nanoparticles on the microstructure and mechanical durability of meltspun lead-free solders based on tin alloys, *J. Alloy Compd.*, 2016, vol. 688, pp. 143–155.
8. Sobhy, M., El-Refai, A.M., Mousa, M.M., and Saad, G., Effect of ageing time on the tensile behavior of Sn–3.5 wt %Ag–0.5 wt % Cu (SAC335) solder alloy with and without adding ZnO nanoparticle, *Mater. Sci. Eng. A*, 2015, vol. 646, pp. 82–89.
9. El-Daly, A.A., El-Hosainy, H., Elmosalami, T.A., and Desoky, W.M., Microstructural modifications and properties of low-Ag-content Sn–Ag–Cu solder joints induced by Zn alloying, *J. Alloy Compd.*, 2015, vol. 653, pp. 402–410.
10. Ramli, M.I.I., Saud, N., Mohd Salleh, M.A.A., and Derman, Mohd Said, M.N., Effect of TiO_2 additions on Sn–0.7Cu–0.05Ni lead-free composite solder, *Microelectron. Reliab.*, 2016, vol. 65, pp. 255–264.
11. Sharif, A., and Chan, Y.C., Effect of indium addition in Sn-rich solder on the dissolution of Cu metallization, *J. Alloy Compd.*, 2005, vol. 390, pp. 67–73.
12. El-Daly, A.A., El-Tantawy, F., Hammad, A.E., Gaafar, M.S., El-Mossalamy, E.H., and Al-Ghamdi, A.A., Structural and elastic properties of eutectic Sn–Cu lead-free solder alloy containing small amount of Ag and In, *J. Alloy Compd.*, 2011, vol. 509, pp. 7283–7246.
13. Lejuste, C., Hodaj, F., and Petit, L., Solid state interaction between a Sn–Ag–Cu–In solder alloy and Cu substrate, *Intermetallics,* 2013, vol. 36, pp. 102–108.
14. Kanlayasiri, K. and Agiga, T., Influence of thermal aging on microhardness and microstructure of Sn–0.3Ag–0.7Cu–*x*In lead-free solders, *J. Alloys Compd.*, 2010, vol. 504, pp. L5–L9.
15. Shalaby, R.M., Influence of indium addition on structure, mechanical, thermal and electrical properties of tin–antimony based metallic alloys quenched from melt, *J. Alloys Compd.*, 2009, vol. 480, pp. 334–339.
16. Negm, S.E., Mady, H., and Bahgat, A.A., Influence of the addition of indium on the mechanical creep of Sn–3.5% Ag alloy, *J. Alloys Compd.*, 2010, vol. 503, pp. 65–70.
17. Lee, H.T., Lee, C.Y., Lee, F.F., Chen, Y.F., and Lee, Y.H., Microstructural evolution of Sn–Ag–Sb solder with indium additions, *J. Electron. Mater.*, 2009, vol.38, pp. 2112–2121.
18. Luo, Z.B., Zhao, J., Gao, Y.J., and Wang, L., Revisiting mechanisms to inhibit Ag_3Sn plates in Sn–Ag–Cu

solders with 1 wt % Zn addition, *J. Alloys Compd.*, 2010, vol. 500, pp. 39–45.

19. Lin, L.W., Song, J.M., Lai, Y.S., Chiu, Y.T., Lee, N.C., and Uan, J.Y., Alloying modification of Sn–Ag–Cu solders by manganese and titanium, *Microelectron. Reliab.*, 2009, vol. 49, pp. 235–241.
20. Fallahi, H., Nurulakmala, M.S., Fallahi Arezodar, A., and Abdullah, J., Effect of iron and indium on IMC formation and mechanical properties of lead-free solder, *Mater. Sci. Eng. A*, 2012, vol. 553, pp. 22–31.
21. Wang, J.X., Yin, M., Lai, Z.M., and Li, X., Wettability and microstructure of Sn–Ag–Cu–In solder, *Trans. China Weld. Inst.*, 2011, vol. 32, pp. 69–73.
22. El-Daly, A.A., Swilem, Y., and Hammad, A.E., Creep properties of Sn–Sb based lead-free solder alloys, *J. Alloys Compd.*, 2009, vol. 471, pp. 98–104.
23. El-Daly, A.A., and Hammad, A.E., Elastic properties and thermal behavior of Sn–Zn based lead-free solder alloys, *J. Alloys Compd.*, 2010, vol. 505, pp. 793–800.
24. Elmer, J.W., Specht, E.D., and Kumar, M., Microstructure and in situ observations of undercooling for nucleation of β-Sn relevant to lead-free solder alloys, *J. Electron. Mater.*, 2010, vol. 39, pp. 273–282.
25. Shnawah, D.A.A., Said, S.B.M., Sabri, M.F.M., Badruddin, I.A.B., and Che, F.X., Microstructure, mechanical, and thermal properties of the Sn–1Ag–0.5Cu solder alloy bearing Fe for electronics applications, *Mater. Sci. Eng. A*, 2012, vol. 551, pp. 160–168.
26. Hammad, A.E., Evolution of microstructure, thermal and creep properties of Ni-doped Sn–0.5Ag–0.7Cu low-Ag solder alloys for electronic applications, *Mater. Des.*, 2013, vol. 52, pp. 663–670.